

Size-dependent yield stress in twinned gold nanowires mediated by site-specific surface dislocation emission

Chuang Deng and Frederic Sansoz^{a)}

School of Engineering and Materials Science program, University of Vermont, Burlington, Vermont 05405, USA

(Received 9 July 2009; accepted 16 August 2009; published online 4 September 2009)

Large-scale molecular dynamics simulations were performed to demonstrate the synergistic effects of twin boundaries and free surfaces on dislocation emission in gold nanowires under tensile loading. It is revealed that the addition of nanoscale twins to crystalline nanowires can act to either increase or decrease their resistance to slip in tension, depending on both sample diameter and number of twins per unit length. Site-specific surface dislocation emission and image forces due to twin boundaries are used to explain the size-dependence of yield stress in twinned gold nanowires. © 2009 American Institute of Physics. [DOI: 10.1063/1.3222936]

Twinning plays a ubiquitous role in the synthesis of thin films and nanowires (NWs) and their mechanical properties.¹ Coherent twin boundaries (CTBs) on (111) atomic planes have been observed in various metallic nanomaterials such as nanocrystalline stainless-steel and Cu films,^{2–4} and single-crystal NWs in Au, Ag, and Cu.^{5–8}

Recent fundamental progress has been made to comprehend the complex interactions between slip and pre-existing twin boundaries in bulk metallic crystals under external loading.^{9–13} Furthermore, it has been found that the necessary stress for dislocation nucleation is critical to determine whether CTBs strengthen NWs via dislocation-twin interactions.¹⁴ However, a predictive understanding of twin boundary effects on the onset of plastic yielding in low-dimensional metals remains elusive, primarily because past molecular dynamics (MD) simulations have predicted different trends in terms of microstructure dependence on yield stress in twinned NWs. More specifically, Hyde *et al.*¹⁵ have calculated that the stress required to nucleate new dislocations under tension in Au NWs with diameters ranging from 5–17.5 nm was 18%–22% less by introducing one CTB, in comparison to that of a perfect single-crystal NW with corresponding diameter. On the contrary, MD simulations on 5-nm-square NWs in Cu¹⁶ and 12-nm-diameter circular pillars in Au^{1,17} have shown evidence that the addition of nanoscale twins could act to increase the stress for dislocation nucleation as the twin density increases (or, inversely, the spacing between twin planes decreases). In the latter study, however, it was also found that CTBs played no role on mechanical properties when the twin boundary spacing (TBS) was larger than or equal to the pillar diameter.

The aim of this letter is to resolve the apparent discrepancy by investigating the synergistic effects of twin density, sample diameter, and free surface on the plasticity of nano-twinned gold. To this regard, we present a large series of MD simulations revealing that the process of surface-mediated dislocation nucleation is site-specific in twinned gold under tensile loading. We show that, in the absence of free surfaces (i.e., using three-dimensional periodic boundaries), there is no dependence of yield stress on the TBS in simulated bulk gold with perfect (111) CTBs, while twin-size effects be-

come much stronger in twinned Au NWs with decreasing diameter.

MD simulations were performed with an embedded-atom-method potential for gold developed by Grochola *et al.*¹⁸ to determine the tensile yield stress of circular NWs with parallel (111) CTBs as shown in Fig. 1(a). NWs of diameter D , which was varied from 4.1 to 24.6 nm, were modeled by imposing periodic boundary conditions along the [111] wire axis, while all other directions were kept free. We

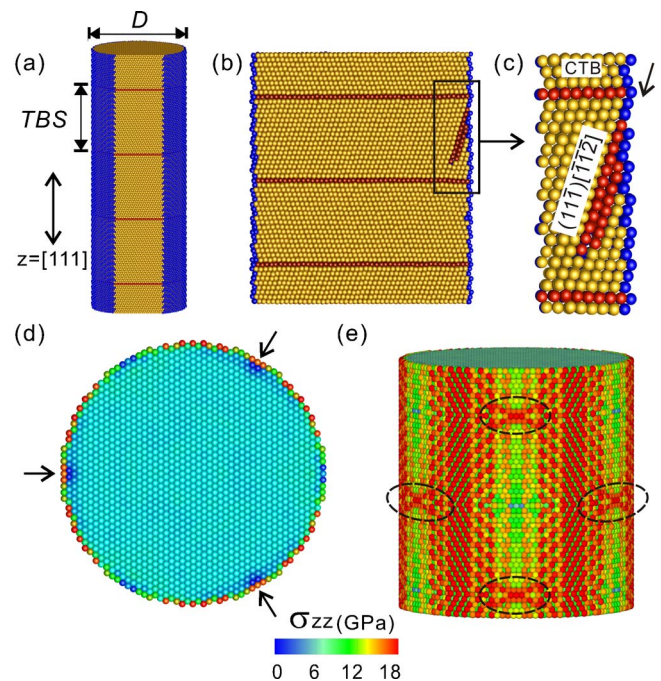


FIG. 1. (Color online) Crystal slip under tension mediated by site-specific surface dislocation nucleation in perfectly circular [111]-oriented Au nanowires containing a periodic arrangement of (111) CTBs. (a) Atomistic structure of a twinned Au nanowire. The nanowire front is cut to show the interior structure. (b) Emission of the very first partial dislocation along a $\{111\}$ glide plane where a CTB intersects the free surface in a nanowire deformed at 300 K. (c) Close-up view on the dislocation nucleation site. Atoms are colored according to the crystal structure. Local distributions of (d) tensile stresses on the twin boundary plane and (e) tensile stresses on the wire surface of a twinned Au nanowire deformed at 1 K ($z=[111]$). Arrows and dashed circles in (d) and (e), respectively, mark the position of dislocation nucleation sites present on the free surface.

^{a)}Tel.: (802) 656 3837. Electronic mail: frederic.sansoz@uvm.edu.

constructed NWs with an initial periodic length equal to 33.6 nm. The simulations were performed at 300 and 1 K by following the same procedure as in Ref. 19 at a constant tensile strain rate of $2.7 \times 10^7 \text{ s}^{-1}$. The analysis of Ackland and Jones²⁰ was used to obtain snapshots of the crystal structure during deformation. Stress calculations were conducted according to the Virial theorem.²¹

A key result found in our MD simulations on NWs is that the dislocation nucleation process is surface-mediated and site-specific. By way of illustration, we show in Fig. 1(b) the snapshot of a twinned NW after its elastic limit has been reached at 300 K. In this figure, elastic limit and plastic yielding in the NW take place via the emission of $(11\bar{1})[112]$ partial dislocations emanating from the free surface, which is consistent with the mechanisms observed experimentally by electron microscopy in nanotwinned Cu.²² A close-up view of the nucleation site in Fig. 1(c) shows that this dislocation precisely propagates on the $(11\bar{1})$ glide plane where a CTB intersects the free surface.

The local analysis of atomic stresses at 1 K, a few steps before yielding, is presented in Figs. 1(d) and 1(e) for comparison. Figure 1(d) shows that the dislocation nucleation sites in each CTB plane are localized in three zones corresponding to the intersection of the CTB with three $\{11\bar{2}\}$ planes on the wire surface. Snapshots of deformation several steps later confirmed that the yielding of this NW at 1 K is associated with the emission of three partial dislocations simultaneously from these sites (not shown). It is important to note however that at 300 K, not all partial dislocations from these sites were nucleated at the same time. Figure 1(e) reveals that each nucleation site exhibits relatively higher tensile stresses on the wire surface than that of most surface atoms. Furthermore, a top view of the twin plane in Fig. 1(d) indicates that the tensile stress near each nucleation site becomes significantly smaller than the rest inside the wire over a distance equal to two atom layers. Therefore, this observation points to a possible yield criterion in twinned Au NWs as follows. The dislocation nucleation proceeds from sites of stress concentration on the free surface where the highest stress gradient is achieved, which is consistent with the general criterion for dislocation nucleation in nanoscale crystalline volumes proposed earlier by Miller and Acharya.²³ We also noticed that the stress level is higher at 1 K than at 300 K in the same Au NW at yield point, which is due to the lack of thermal activation at 1 K.

Another essential result is that without free surfaces, nanoscale twins alone are found to have no intrinsic influence on the yielding behavior of gold. For example, Fig. 2 represents the evolution of the critical resolved shear stress (CRSS) as a function of number of twins per unit length, $1/\text{TBS}$, in a bulk material simulated by MD using a cubic model with periodic boundaries applied along all spatial axes (see inset in Fig. 2). The CRSS calculations were obtained by deforming the simulation box at constant strain rate ($5 \times 10^7 \text{ s}^{-1}$) along the $[111]$ axis with zero pressure exerted on the lateral directions using NPT integration, N is the number of atoms, P is the pressure, and T is the temperature, and assuming a Schmid factor of 0.314, which corresponds to the propagation of partial dislocations in the $\{11\bar{1}\}\langle 112 \rangle$ slip system. This figure reveals that the bulk behavior is not affected by the TBS, which stems from the fact that the dislocation

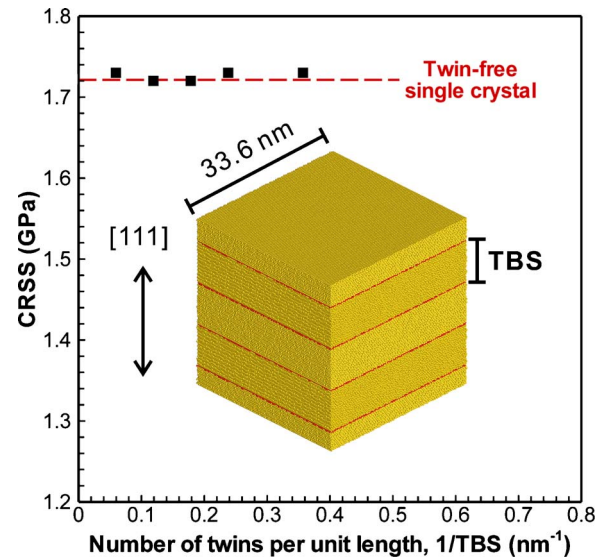


FIG. 2. (Color online) Change in the CRSS for dislocation nucleation as a function of the number of twin boundaries per unit length, $1/\text{TBS}$, in simulated $[111]$ -oriented bulk gold under tension. The horizontal dashed line represents the CRSS value obtained in a twin-free sample of same size and geometry.

nucleation process is homogeneous, as opposed to surface-mediated, in this case. Furthermore, the CRSS for both twinned and twin-free single-crystal models are almost identical ($\sim 1.72 \text{ GPa}$), which is in good agreement with past atomistic predictions²⁴ of ideal yield strength for the shearing of two Au $\{111\}$ planes in $\langle 112 \rangle$ directions (1.78 GPa).

In contrast, the MD results presented in Fig. 3 show clear evidence that strong size effects exist in twinned Au NWs. First, the curves show a linear dependence of the CRSS for dislocation nucleation as a function of $1/\text{TBS}$. Second, as shown in the inset of Fig. 3, the slope of this scaling behavior increases

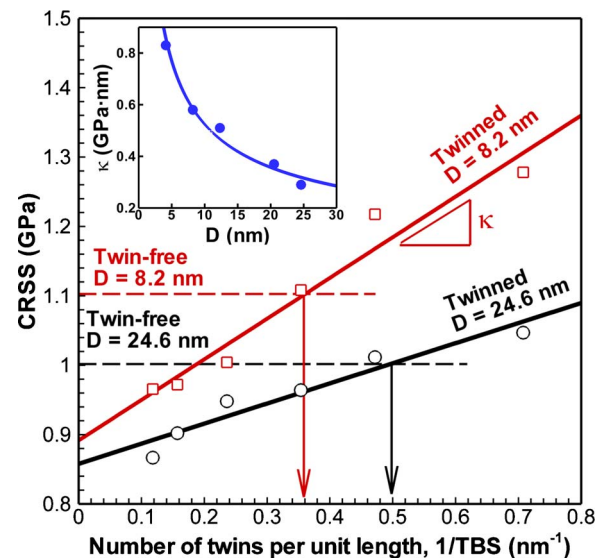


FIG. 3. (Color online) Change in the CRSS for dislocation nucleation as a function of the number of twin boundaries per unit length, $1/\text{TBS}$, in simulated gold nanowires with diameters equal to 8.2 and 24.6 nm at 300 K. A mechanical transition from twin-induced weakening to strengthening regimes is indicated by a vertical arrow. The inset shows the change in the slope κ of the fitted line as a function of nanowire diameter D varying from 4.1 to 24.6 nm.

with decreasing NW diameter D . As a result of the twin-size dependency, the yielding behavior of twinned Au NWs can be divided into weakening and strengthening regimes with respect to the CRSS obtained in twin-free NWs deformed under the same condition. NWs with low number of twins (or large TBS) yield at smaller stress than that predicted in twin-free samples of same geometry and size, and at larger stress when the number of twins per unit length exceeds a critical limit. For example, Fig. 3 shows that the transition from weakening to strengthening regimes occurs when TBS is equal to 2.78 and 2.02 nm in twinned Au NWs with diameters of 8.2 and 24.6 nm, respectively.

We also found that dislocation emission in twinned Au NWs with a nonuniform distribution of CTBs (not shown here) always occurs on the CTB associated with the largest TBS. For example, when $D=8.2$ nm, the yield stress for a NW containing nine CTBs with TBS=2.8 nm and only one CTB with TBS=8.4 nm is 3.12 GPa, which is very close to that of a periodically twinned NW with TBS=8.4 nm (3.08 GPa), while that of a periodically twinned NW with TBS=2.8 nm is equal to 3.53 GPa. This result enables us to conclude that the dislocation nucleation process is directly correlated with the largest distance between two twin boundaries, rather than the twin density.

The above results can be interpreted using the two-phase model of Chen *et al.*¹⁰ who have calculated the image shear stress τ_{CTB} exerted by a (111) CTB on the glide of a full dislocation in twinned systems with free boundaries. They predicted that the dislocation-CTB interaction force is repulsive at large distances (i.e., $>3b$ with b the magnitude of the Burgers vector), due to the elasticity mismatch between parent and twin grains in terms of shear modulus across the CTB, such that

$$\tau_{\text{CTB}} = \frac{\lambda\mu b}{4\pi x}, \quad (1)$$

where x is the distance between the dislocation and the CTB, λ is a dimensionless measure of the intrinsic strength of the CTB, and μ is the shear modulus along the slip system. A caveat however is that the theory of Chen *et al.*¹⁰ is based on the interaction of CTBs with pure screw dislocations of infinite length, as opposed to curved dislocation lines such as those observed here when partial dislocations are emitted from the surface of circular Au NWs. We thus propose to scale Eq. (1) with a factor $f(D)$ in order to account for the curvature of these dislocations, which is also a function of the NW diameter D .²⁵ Assuming here that x represents the distance between a dislocation nucleation site at the intersection of a CTB with the free surface and the closest CTB, we have $x=\text{TBS}/\sin\theta$ with θ the angle between the glide plane and the CTB. The CRSS obtained in twinned Au NWs can therefore be written as

$$\text{CRSS} = \tau_0 + \tau_{\text{CTB}} = \tau_0 + \frac{\lambda\mu b \sin\theta}{4\pi\text{TBS}} f(D), \quad (2)$$

where τ_0 is the CRSS in twinned Au NWs with TBS near infinity, which is lower than that in twin-free single-crystal Au NWs.¹⁵ The atomistic results presented in Fig. 3 for two

diameters give credence to the linear dependence between CRSS and $1/\text{TBS}$, and the transition from weakening to strengthening regime with decreasing TBS as obtained in Eq. (2). The inset of Fig. 3, which shows the increase in slope for the CRSS- $1/\text{TBS}$ relationship with decreasing diameter, also supports the evolution of $f(D)$. Determining a closed form for $f(D)$ is beyond the scope of this paper.

In summary, MD simulations of tension of twinned Au NWs with circular cross-section have revealed that the incipient plasticity mechanisms proceed via the nucleation and emission of partial dislocations from specific sites where CTBs intersect $\{11\bar{2}\}$ planes on the free surface. Prior to dislocation emission, these sites possess significantly higher stress gradients than the rest of the specimen. The simulations support the idea that the addition of CTBs to crystalline NWs could cause strengthening effects, weakening effects, and no effects, as a function of both twin spacing and sample diameter. Such a model can be used to reconcile the conflicting observations made in the past on the twin-dependency of yield stress in twinned NWs.

Support from NSF CAREER program (Grant No. DMR-0747658) and the computational resources provided by the Vermont Advanced Computing Center (NASA Grant No. NNX06AC88G) are gratefully acknowledged. The simulations shown in this work were performed using LAMMPS (Ref. 26).

¹F. Sansoz, H. Huang, and D. H. Warner, *JOM* **60**, 79 (2008).

²L. Lu, Y. Shen, X. Chen, L. Qian, and K. Lu, *Science* **304**, 422 (2004).

³X. Zhang, H. Wang, X. H. Chen, L. Lu, and K. Lu, *Appl. Phys. Lett.* **88**, 173116 (2006).

⁴O. Anderoglu, A. Misra, H. Wang, F. Ronning, M. F. Hundley, and X. Zhang, *Appl. Phys. Lett.* **93**, 083108 (2008).

⁵M. Tian, J. Wang, J. Kurtz, T. E. Mallouk, and M. H. W. Chan, *Nano Lett.* **3**, 919 (2003).

⁶J. Wang, M. Tian, T. E. Mallouk, and M. H. W. Chan, *J. Phys. Chem. B* **108**, 841 (2004).

⁷J. Wang, H. Huang, S. V. Kesapragada, and D. Gall, *Nano Lett.* **5**, 2505 (2005).

⁸B. Wu, A. Heidelberg, J. J. Boland, J. E. Sader, X. Sun, and Y. Li, *Nano Lett.* **6**, 468 (2006).

⁹Z. H. Jin, P. Gumbsch, E. Ma, K. Albe, K. Lu, H. Hahn, and H. Gleiter, *Scr. Mater.* **54**, 1163 (2006).

¹⁰Z. Chen, Z. Jin, and H. Gao, *Phys. Rev. B* **75**, 212104 (2007).

¹¹T. Zhu, J. Li, A. Samanta, H. G. Kim, and S. Suresh, *Proc. Natl. Acad. Sci. U.S.A.* **104**, 3031 (2007).

¹²Z. H. Jin, P. Gumbsch, K. Albe, E. Ma, K. Lu, H. Gleiter, and H. Hahn, *Acta Mater.* **56**, 1126 (2008).

¹³L. Li and N. M. Ghoniem, *Phys. Rev. B* **79**, 075444 (2009).

¹⁴Y. Zhang and H. Huang, *Nanoscale Res. Lett.* **4**, 34 (2009).

¹⁵B. Hyde, H. D. Espinosa, and D. Farkas, *JOM* **57**, 62 (2005).

¹⁶A. J. Cao, Y. G. Wei, and S. X. Mao, *Appl. Phys. Lett.* **90**, 151909 (2007).

¹⁷K. A. Afanasyev and F. Sansoz, *Nano Lett.* **7**, 2056 (2007).

¹⁸G. Grochola, S. P. Russo, and I. K. Snook, *J. Chem. Phys.* **123**, 204719 (2005).

¹⁹C. Deng and F. Sansoz, *Nano Lett.* **9**, 1517 (2009).

²⁰G. J. Ackland and A. P. Jones, *Phys. Rev. B* **73**, 054104 (2006).

²¹J. Diao, K. Gall, and M. L. Dunn, *J. Mech. Phys. Solids* **52**, 1935 (2004).

²²Y. B. Wang, B. Wu, and M. L. Sui, *Appl. Phys. Lett.* **93**, 041906 (2008).

²³R. E. Miller and A. Acharya, *J. Mech. Phys. Solids* **52**, 1507 (2004).

²⁴K. Gall, J. Diao, and M. L. Dunn, *Nano Lett.* **4**, 2431 (2004).

²⁵J. R. Greer and W. D. Nix, *Phys. Rev. B* **73**, 245410 (2006).

²⁶S. J. Plimpton, *J. Comput. Phys.* **117**, 1 (1995).